Mn doped hard type perovskite high-temperature BYPT–PZN ternary piezoelectric ceramics

Yunli Wang [a], Kai Cai [b], Feng Jiang [a], Junying Zhang [c], Dong Guo [a],*

[a] *Institute of Acoustics, Chinese Academy of Sciences, Beijing 100190, China*
[b] *Beijing Center for Chemical and Physical Analysis, Beijing 100089, China*
[c] *Beihang University, Department of Physics, Ministry of Education, Key Laboratory of Micro-Nano Measurement-Manipulation & Physics, Beijing 100191, China*

ARTICLE INFO

ABSTRACT

The undoped perovskite type high Curie temperature (T_c) piezoelectric ceramics usually show a rather low mechanical quality factor (Q_m) with low energy conversion efficiency. In this study, the microstructure and electric properties of Mn doped new perovskite ternary high Curie temperature piezoelectric ceramic system BYPT–PZN–xMn were investigated. After the addition of Mn, the Q_m of the system was significantly increased, while the piezoelectric performance showed only a slight decrease. At a Mn content of 1.00 mol%, the ceramic showed a Q_m of more than 1200, which is about one order of magnitude higher than those of other perovskite type high Curie temperature piezoelectric ceramics, implying a low energy loss of the material. Mn addition also enhanced the T_c of the system, and the depolarization temperature derived from high temperature d_{33} measurement of the sample with the best overall performance was higher than 300 °C. The improved performance is attributed to the improved density and poling efficiency as well as the 'acceptor' type doping effect of Mn.

1. Introduction

In recent years, piezoelectric ceramics with a Curie temperature (T_c) higher than that of the conventional PZT ($T_c \approx 320–370$ °C) have received a great deal of attention for application in sensors and actuators working at elevated temperatures, particularly, for aerospace and automotive industries [1]. Under-hood automotive applications such as internal vibration sensors or active fuel injection nozzles require operation temperatures as high as 300 °C, while aerospace and aircraft industries require a much higher operation temperature. The commercial PZT ceramics generally have a T_c much less than 380 °C. The corresponding operating temperatures are generally limited to a half of this value due to the deteriorated polarization with increasing temperature. The available piezoelectric materials with a higher T_c usually show a worse piezoelectric property [1,2]. For example, lead metaniobate has a T_c of about 570 °C, but its d_{33} is only about 80 pC/N, and it requires a complicated fabrication procedure to get dense and homogeneous samples [3]. A certain lead free system also shows both a high T_c

($\sim$420 °C) and a high d_{33} ($\sim$200 pC/N) [4], while the evaporation of sodium or potassium during sintering and some other processing problems make it rather difficult to get dense products with stable performance. Among the many types of high T_c piezoelectric ceramics, the solid solution $(1-x)$BiScO$_3$–xPbTiO$_3$ (BSPT) with a perovskite structure seems to be a very attractive one due both to its high T_c of $\sim$450 °C and high d_{33} of $\sim$460 pC/N near the morphotropic phase boundary (MPB) at $x = 0.64$ [5]. High T_c and high piezoelectric response were also achieved for similar perovskite systems with the general form BiMeO$_3$–PbTiO$_3$ (BMePT), where Me can be a single or mixture of cations with an average valence of +3. However, the high cost of the raw material Sc$_2$O$_3$ and the very low mechanical quality factor (Q_m) of BMePT type materials severely limit their application for high power devices [6]. The Q_m values are rarely reported and the available data are generally less than 100 (a value one or two orders of magnitude lower than that of PZT), which means a rather large dissipated energy in electromechanical systems. Therefore, scandium-free complex perovskite high temperature piezoelectric ceramics with a much higher Q_m are highly desirable [6–9]. Among the BMePT type piezoelectric ceramics, BiYbO$_3$–PbTiO$_3$ (BYPT) has a high T_c up to 630 °C, but it has a very low d_{33} ($\sim$28 pC/N) and a low structural stability due to the large difference in tolerance factor of BiYbO$_3$ ($\sim$0.863) and PbTiO$_3$ ($\sim$1.02) [5,10,11]. We found that the piezoelectric properties and

* Corresponding author. Tel.: +86 1082547679; fax: +86 1082547677.
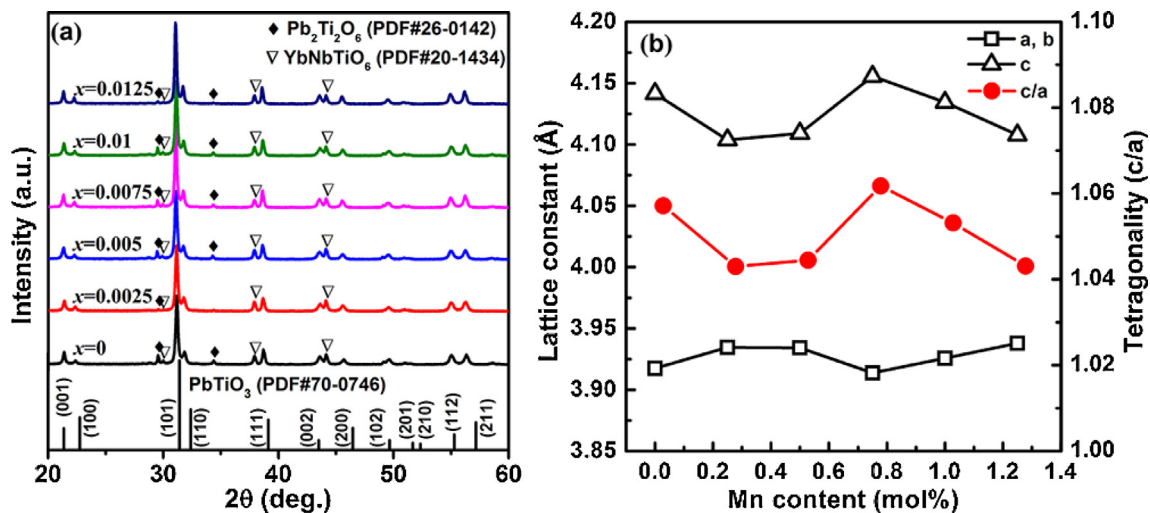 *E-mail addresses:* dong.guo@mail.ioa.ac.cn, guodong99@tsinghua.org.cn (D. Guo).

Fig. 1. (a) XRD patterns of various BYPT–PZN–xMn ceramic samples; (b) Mn content dependence of lattice constants and tetragonality.

material stability of BYPT could be improved by adding another component with a low tolerance factor such as PZN. However, the ternary system BYPT–PZN still has a low Q_m [12]. In this study, the variable doping element Mn was selected as a dopant due to its multiple modification effects, and the microstructure and electrical properties of Mn doped BYPT–PZN system with a composition of $0.6(0.1BiYbO_3–0.9PbTiO_3)–0.4Pb(Zn_{1/3}Nb_{2/3})O_3$ possessing the optimum performance [12] were investigated. It was found that, suitable amount of Mn could not only significantly improve the hardness, but could also improve the T_c without obvious effect on the piezoelectric properties of the material. This could be explained by the improved density, higher poling efficiency, and the 'acceptor' type doping effect of Mn.

2. Experimental

The general formulation of the material in this study is $0.6(0.1BiYbO_3–0.9PbTiO_3)–0.4Pb(Zn_{1/3}Nb_{2/3})O_3–xMn$, and this formulation was decided from preliminary experiments. For simplicity, hereafter the system is referred to as BYPT–PZN–xMn. The ceramics were prepared by the columbite precursor method. First, analytically pure ZnO and Nb2O5 were mixed by ball-milling and calcined at 1100 °C for 2 h to produce the ZnNb2O6 precursor. Then the precursor was mixed with analytically pure Bi$_2$O$_3$, YbO$_2$, MnCO$_3$, Pb$_3$O$_4$ and TiO$_2$ according to the stoichicomatic ratio (with 1 wt% excess amounts of Pb$_3$O$_4$) and thoroughly ball-milled, dried, grinded, and calcined at 750 °C for 2 h. The final powders were pressed into pellets, and ceramic samples with a diameter of 10 mm and a thickness of ~1 mm were obtained after debinding at 600 °C and sintering at 1100 °C for 3 h. X-ray diffraction (XRD) profiles were recorded by a Bruker D8 Advance diffractometer with Cu Kα1 radiation. The morphology of the fresh fractured surfaces of the samples was examined by scanning electron microscopy (SEM, Hitachi S-4800, Japan). The samples for electrical measurement were pasted with silver electrode and poled at 170 °C for 20 min under an electric field of 4 kV/mm in a silicone oil bath after 24 h aging. The mechanical quality factor (Q_m) were measured by using the resonance and anti-resonance method with
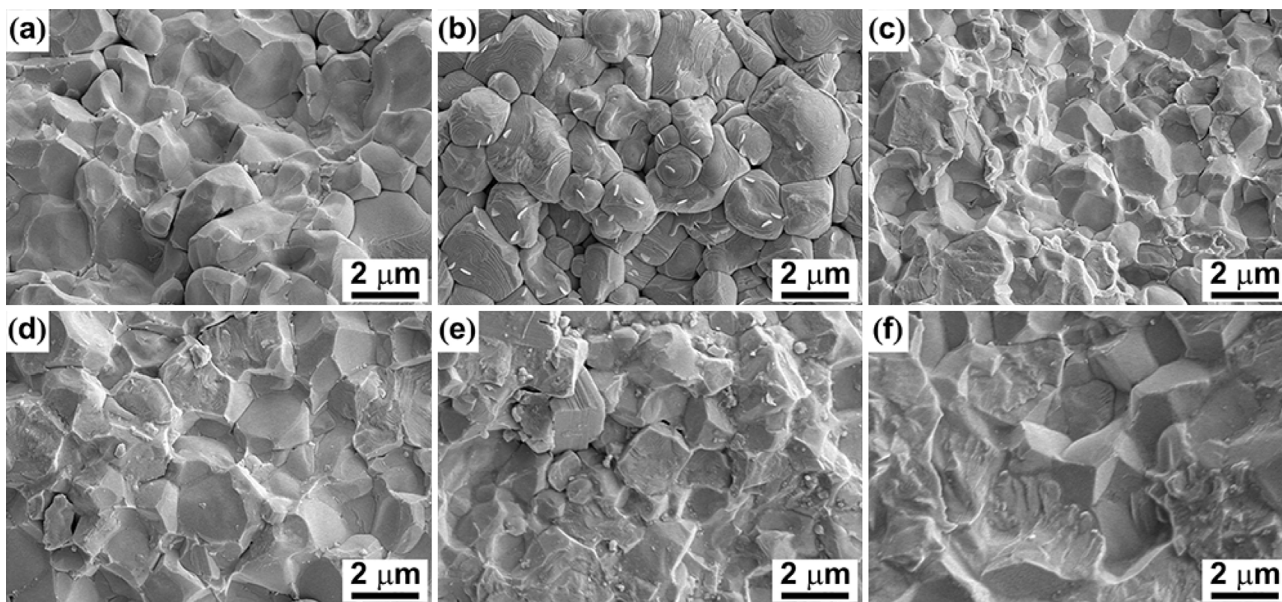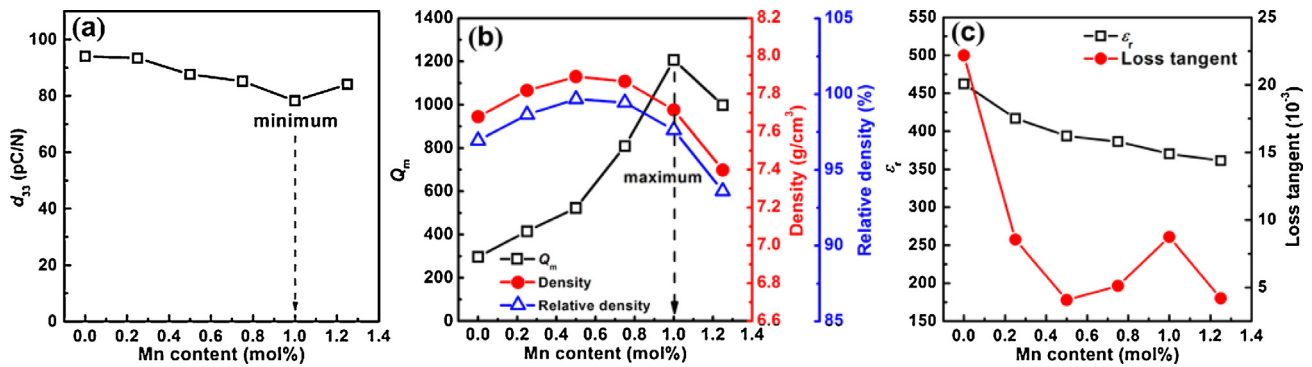

Fig. 2. SEM images showing the morphology of different BYPT–PZN–xMn ceramic samples: (a)–(f) are the images for samples with an x value of 0, 0.0025, 0.005, 0.0075, 0.01, and 0.0125, respectively.

Fig. 3. Mn content dependence of piezoelectric coefficient d_{33} (a), Q_m, density and relative density (b), and room temperature ε_r and loss tangent (1 kHz) (c) of various BYPT–PZN–xMn ceramic samples.

an HP4294A impedance analyzer. The temperature dependence of dielectric constant ε_r was measured at 1 kHz using unpoled samples. The high temperature d_{33} was directly measured by the Berlincourt method through a modified ZJ-3DHT quasistatic piezoelectric type d_{33}-meter (Institute of Acoustics, Chinese Academy of Sciences) equipped with a high temperature sample chamber and a Pt/Rh thermalcouple. The polarization hysteresis loops were measured using a Radiant Precision LC ferroelectric testing system. A HP4140B pA Meter equipped with a HP16055A Test Fixture was used to measure the DC current (100 V), then the resistivity (ρ, Ωcm) was calculated according to the cross sectional area and the thickness of the sample.

3. Results and discussion

As can be seen from Fig. 1(a), the XRD patterns of all samples show a perovskite main phase. Although all the peaks of each pattern slightly shift to lower 2θ angle, the patterns correspond well to the $PbTiO_3$ (PDF#70-0746) phase with a typical tetragonal symmetry, showing splitted (001)/(100), (101)/(110), (002)/(200) and (112)/(211) diffractions. Meanwhile, the impurities $Pb_2Ti_2O_6$ (PDF#26-0142) pyrochlore phase and $YbNbTiO_6$ phase (PDF#20-1434) can be identified for all samples. The Mn content dependence of lattice constant and tetragonality (c/a) calculated from the interplanar distance d derived from the XRD patterns are shown in Fig. 1(b). The tetragonality first decreases and then reaches a maximum at a Mn content of 0.75 mol%, where the tetragonality (1.062) is as high as that of the tetragonal phase $PbTiO_3$ (1.063). A higher tetragonality generally means a higher polarization and lattice deformation, while it may cause difficulty in polarization reversal [13]. The appearance of $Pb_2Ti_2O_6$ pyrochlore phase and $YbNbTiO_6$ phase is a problem of the ternary system, because they may affect the electrical performance. From a careful check of the XRD patterns one may find that the intensity of the peaks corresponding to $Pb_2Ti_2O_6$ phase and $YbNbTiO_6$ phase show a decreasing trend with increasing Mn content. This indicates that addition of Mn can suppress the formation of impurity phase.

The SEM images of the samples are shown in Fig. 2. All samples have similar grain size. When the Mn content is larger than 0.50 mol%, the samples show a largely transgranular fractured morphology. Except for the $x = 0.0025$ sample, all samples have a polygonal grain shape with relatively sharp grain boundaries. In comparison, the $x = 0.0025$ sample shows the most distinct morphology. Its grains have a curved shape and contain irregularly but homogeneously distributed smaller lamellar grains, which may indicate the segregation of the impurity phase, probably the $YbNbTiO_6$ phase as revealed by the XRD patterns. The absence of such lamellar grains in other samples may indicate that the

impurity phase has formed homogenous solid solution with the main tetragonal phase.

The Mn content dependence of various electrical parameters of the samples is shown in Fig. 3. As shown in Fig. 3(a), with increasing Mn content, the d_{33} value decreases slightly and reaches a minimum of about 78.2 pC/N at an Mn content of 1.00 mol%. In contrast, with increasing Mn content, the Q_m value shown in Fig. 3(b) increases substantially, and at a Mn content of 1.00 mol% it reaches a maximum of 1207, then it decreases to 997.5. Generally, d_{33} and Q_m of a system show a tradeoff relationship at different dopant concentrations. The results here demonstrate that the Q_m of this ternary system can be substantially improved by Mn doping while the piezoelectric performance remains unchanged. Comparing the Q_m curve with the density and relative density curves, it is not difficult to find that the Q_m change can be partly explained by the density, despite that the two curves still show a large discrepancy in the maximum value position. This is because a dense structure usually facilitates the electromechanical energy conversion, giving rise to reduced energy dissipation. Also, it can be seen from Fig. 3(c) that after addition of Mn, the dielectric constant and the dielectric loss are reduced. These results indicate that Mn have a hard type doping effect in the ternary BYPT–PZN system. A plot of Q_m and d_{33}
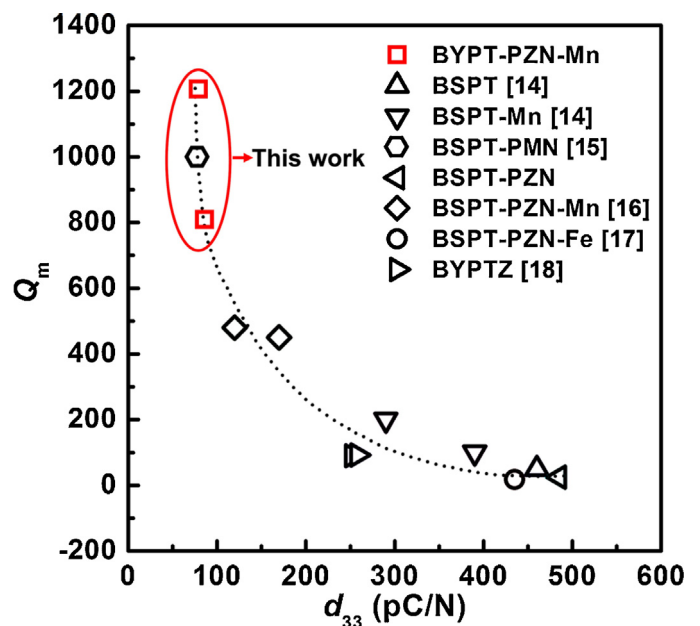
Fig. 4. Schematic illustration of Q_m and d_{33} data of some perovskite piezoelectric ceramics with a T_c higher than 380 °C. The data are from the references as listed within the square brackets in the figure.
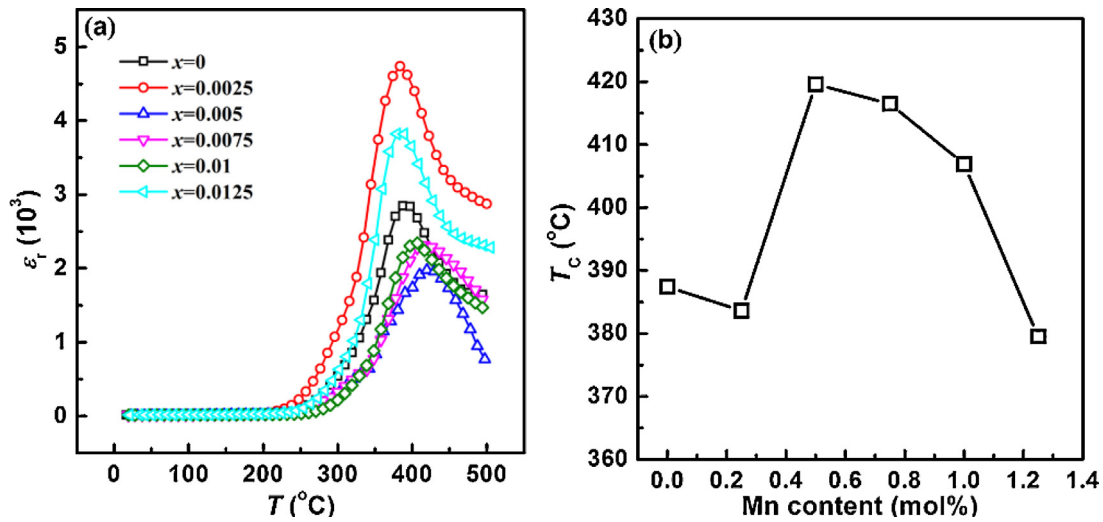
Fig. 5. Temperature dependence of dielectric constant (ε_r, 1 kHz) (a) and Mn content dependence of T_c (b) for various BYPT–PZN–xMn samples.

data of some perovskite high T_c piezoelectric ceramics is schematically illustrated in Fig. 4 [14–18]. Also, BSPT–PZN ceramic sample was fabricated by the similar solid reaction method and its data is listed in the figure to ease the comparison with the data in the literature of the doped BSPT–PZN samples. Although the ceramic materials have very different composition, an inverse proportional relationship of the two parameters is clear from the figure. The data in this study fill up the left side of the curve with the highest

Q_m. The plot may provide some hints on getting high temperature piezoelectric ceramics with properties suitable for a certain application. The figure also shows that doping or formation of complex system containing PT phase is necessary to tailor the performance of high T_c piezoelectric ceramics.

The temperature dependence of dielectric constant (ε_r) of the BYPT–PZN–xMn samples is shown in Fig. 5(a). In the tested temperature range, all the samples show a single dielectric constant
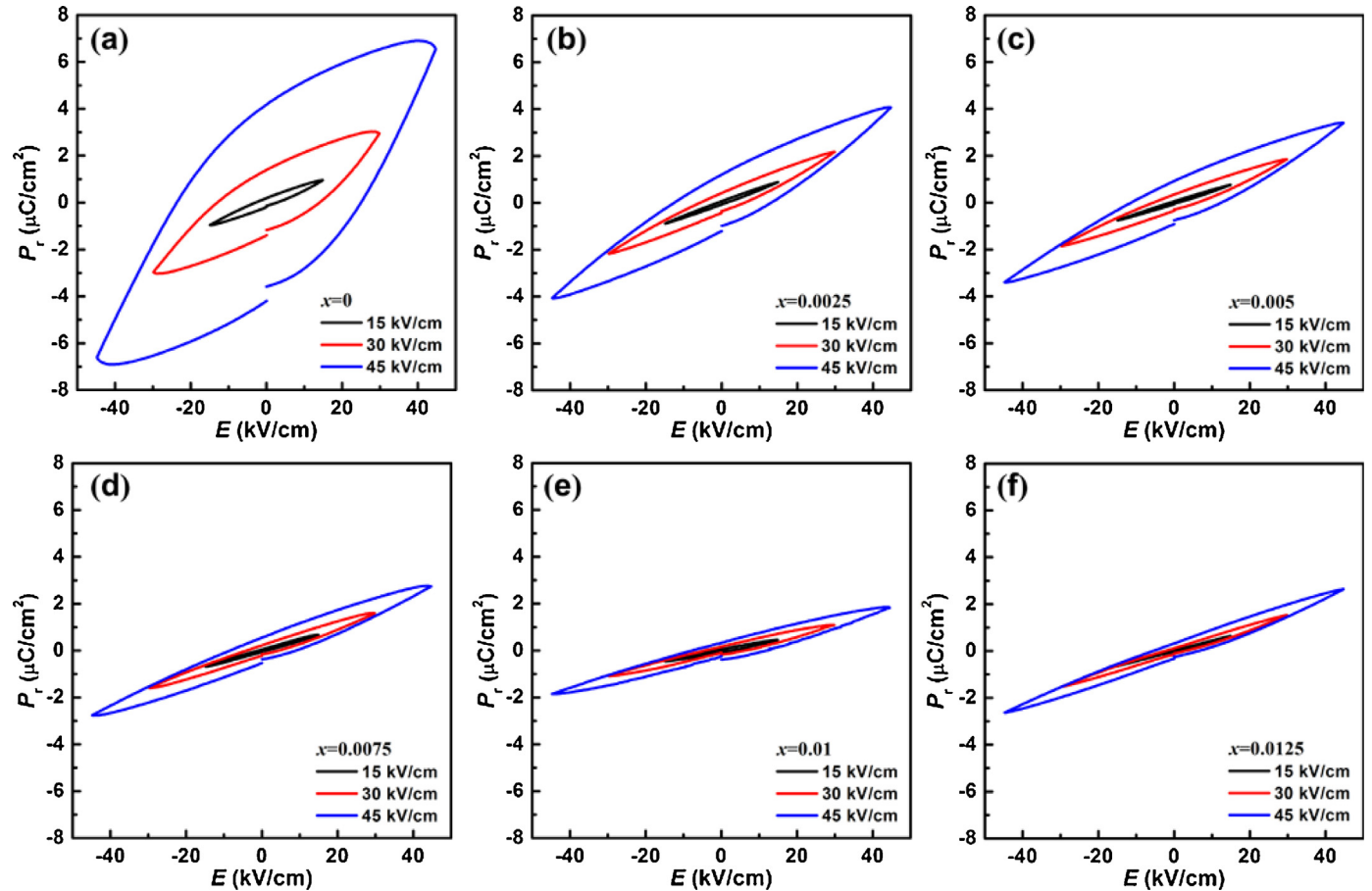

Fig. 6. (a)–(f) are the ferroelectric hysteresis loops under three different electric fields for BYPT–PZN–xMn ceramic samples with an x value of 0, 0.0025, 0.005, 0.0075, 0.01, and 0.0125, respectively.
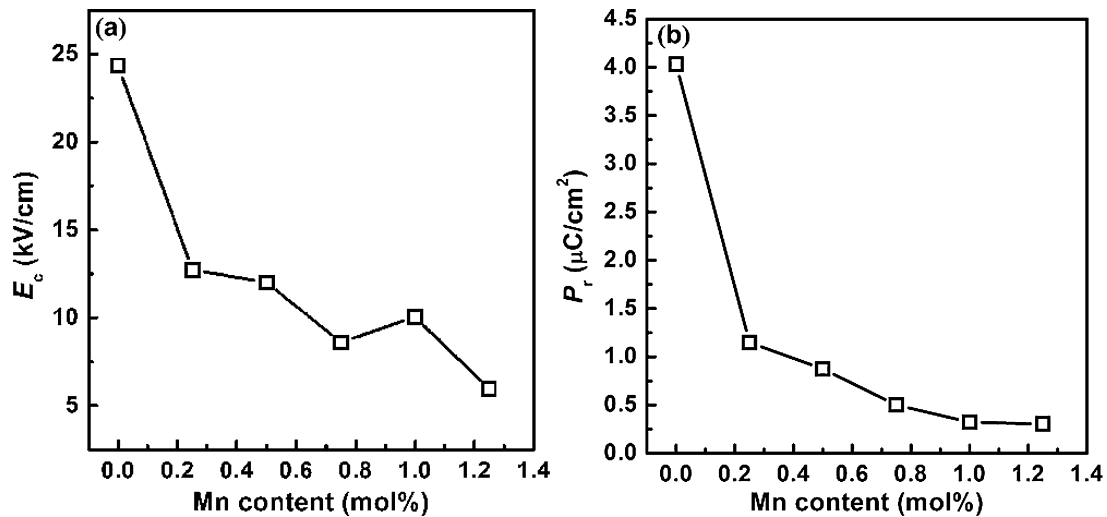
Fig. 7. Mn content dependence of E_c (a) and P_r (b) derived from the hysteresis loops (45 kV/cm) of various BYPT–PZN–xMn ceramic samples.

peak that is due to the ferroelectric–paraelectric phase transition. Accordingly, the Mn content dependence of T_c is derived as shown in Fig. 5(b). With increasing Mn content, T_c first keeps almost unchanged, and then it increases significantly from 383.6 °C to a maximum of 419.6 °C at a Mn content of 0.50 mol% which is about 32.2 °C higher than that of the undoped sample. Following that it decreases again. The curve indicates that suitable amount of Mn can enhance the T_c of the system. Comparing Fig. 5(b) with the Mn content dependence of tetragonality shown in Fig. 1(b), one may find that the two curves show a certain similarity except for the point at $x = 0.5$. A deviation point is not unusual as a doping element generally has a complicated influence on the interactions of the ions in ceramics. Thus, the change in T_c may be partly explained by the changed tetragonality [19].

The ferroelectric–electric field hysteresis loops of the BYPT–PZN–xMn samples are shown in Fig. 6(a)–(f). The shapes of all loops are far from saturation. The undoped BYPT–PZN sample shows an open loop, while Mn doping gives rise to rather slim loops, as reflected from the decreased E_c with increasing Mn content shown in Fig. 7(a). From the Mn content dependent remnant polarization (P_r) values derived from the loops as shown Fig. 7(b), it is clear that addition of Mn largely reduced the P_r, implying that the polarization in the BYPT–PZN system may be seriously refrained. This again indicates that Mn should have a hard doping effect. According to the electrostrictive coupling relationship $d_{33} = 2\varepsilon_{33}Q_{33}P_r$, where Q_{33} is the electrostrictive coefficient [2], and ε_{33} is the dielectric constant, a more or less decreased d_{33} should be obtained as a consequence of the decreased P_r. The d_{33} values shown in Fig. 3(a) are indeed decreased, but in general the d_{33} is not so largely affected despite the significant decrease in P_r. An explanation for this might be the improved poling efficiency, as Mn doping may increase the resistivity and produce trapping centers for injected charges. To confirm this idea we measured the resistivity of the samples. As shown in Fig. 8, the resistivity indeed shows an increasing trend with Mn content. The increased resistivity means a low leaking current during poling, which in turn improve the polarization and counterbalance part of the hard doping effect of Mn.

Mn is a variable valence element, and in this study $MnCO_3$ with Mn^{2+} composition was used as the raw material. However, many studies indicate that Mn^{2+} may oxidize already in air to Mn^{3+} or change to the higher valence state Mn^{4+} in the presence of lead oxide. When Mn^{4+} is present, it may substitute all the B-site ions including Nb^{5+} (0.640 Å, 6-coordinate), Ti^{4+} (0.605 Å,

6-coordinate) in the perovskite lattice due to its similar radius (0.670 Å, 6-coordinate) [20]. Then positively charged oxygen vacancies are formed for charge balance. It is well accepted that the B-site defect may react with the oxygen vacancies to form defect dipoles [21]. These dipoles may orient parallel to the spontaneous polarization direction and give rise to an internal bias field, which is believed to be able to pin the domain wall and inhibit polarization switching, leading to a decreased P_r. The effect of defect dipole is reflected by the constricted loops of the samples with Mn content higher than 0.75 mol% shown in Fig. 6(e) and (f), as the internal bias always leads to a constrained or even double loop [22]. The refrained polarization switching may also explain the decreased dielectric constant and dielectric loss. Therefore, these results indicate that Mn may work as an 'acceptor' dopant for the BYPT–PZN ternary system. What makes Mn useful for this system is that, it significantly improved the Q_m without causing obvious deterioration in piezoelectric properties. This may be related to the improved density and poling efficiency as discussed in the forgoing section. Furthermore, a suitable amount of Mn improves the T_c of the system, which can be partly explained by the tetragonality. The
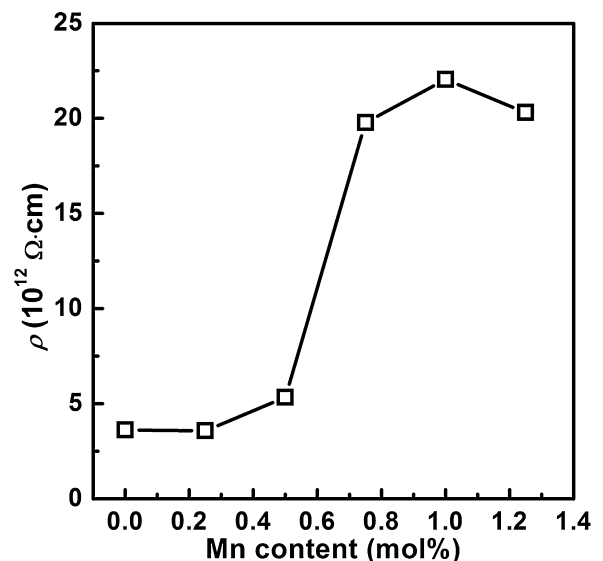

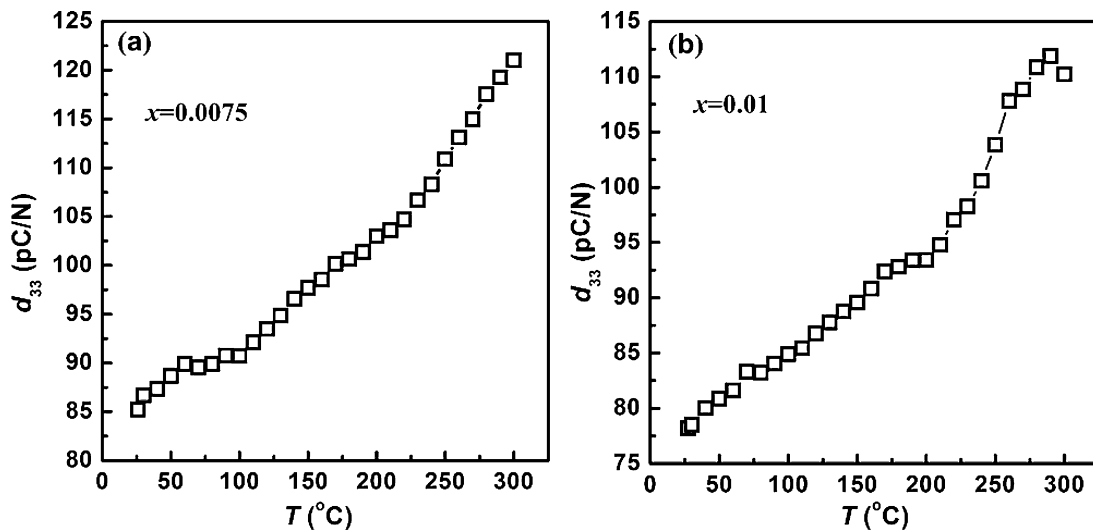**Fig. 8.** Mn content dependence of resistivity of various BYPT–PZN–xMn ceramic samples.

Fig. 9. Temperature dependence of d_{33} of two typical samples directly measured from the Berlincourt method: (a) BYPT–PZN–0.0075Mn, (b) BYPT–PZN–0.01Mn.

BYPT–PZN–0.0075Mn sample seems to be the best sample judging from its overall performance.

To investigate the high temperature piezoelectric properties, the variable temperature d_{33} of the samples were directly measured using a modified d_{33} meter based on the Berlincourt method. As shown in Fig. 9, the d_{33} of the BYPT–PZN–0.0075Mn sample increases monotonously, and depolarization does not occur in the tested temperature range (RT–300 °C). Similar increased d_{33} with increasing temperature were also observed before, which may be interpreted as the instability (profile flattening) of the elastic Gibbs free energy [23] and the increased thermal energy of domains [24]. In comparison, the d_{33} curve of the BYPT–PZN–0.01Mn sample shows a slight roll off at the high temperature side, indicating that too high Mn content gives rise to a lower depolarization temperature. These also imply that the doped BYPT–PZN–xMn sample is suitable for high temperature application.

4. Conclusions

The microstructure and electric properties of Mn doped ternary high temperature piezoelectric ceramic system BYPT–PZN–xMn were studied. After addition of Mn, the mechanical quality factor Q_m of the system was significantly increased, implying a decreased energy dissipation during vibration, while the piezoelectric performance showed only a slight decrease. Suitable amount of Mn also enhanced the T_c of the system. The results indicated that the improved mechanical quality factor could be attributed to the improved density as well as the hard type doping effect of Mn. The optimum properties were obtained for the sample with around 0.75 mol% of Mn, whose Q_m, d_{33} and T_c are 809, 86 pC/N and 416.5 °C, respectively. Direct high temperature d_{33} measurement via the Berlincourt method indicated that depolarization temperature in the sample with the best overall performance was higher than 300 °C.
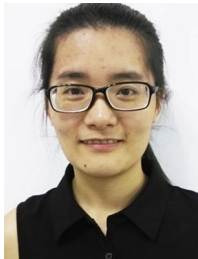
Acknowledgments

References

[1] R.C. Turner, P.A. Fuierer, R.E. Newnham, T.R. Shrout, Materials for high temperature acoustic and vibration sensors: a review, Appl. Acoust. 41 (1994) 299–324.
[2] D. Damjanovic, Materials for high temperature piezoelectric transducers, Curr. Opin. Solid State Mater. Sci. 3 (1998) 469–473.
[3] T.G. Lupeiko, S.S. Lopatin, Old and new problems in piezoelectric materials research and materials with high hydrostatic sensitivity, Inorg. Mater. 40 (2004) S19–S32.
[4] Y.P. Guo, K.I. Kakimoto, H. Ohsato, (Na$_{0.5}$K$_{0.5}$)NbO$_3$–LiTaO$_3$ lead-free piezoelectric ceramics, Mater. Lett. 59 (2005) 241–244.
[5] R.E. Eitel, C.A. Randall, T.R. Shrout, P.W. Rehrig, W. Hackenberger, S.E. Park, New high temperature morphotropic phase boundary piezoelectrics based on Bi(Me)O$_3$–PbTiO$_3$ ceramics, Jpn. J. Appl. Phys. 40 (2001) 5999–6002.
[6] S.J. Zhang, R. Xia, L. Lebrun, D. Anderson, T.R. Shrout, Piezoelectric materials for high power, high temperature applications, Mater. Lett. 59 (2005) 3471–3475.
[7] T.Y. Ansell, D.P. Cann, High temperature piezoelectric ceramics based on $(1 − x)$[BiScO$_3$ + Bi(Ni$_{1/2}$Ti$_{1/2}$)O$_3$]–xPbTiO$_3$, Mater. Lett. 80 (2012) 87–90.
[8] R.R. Duan, R.F. Speyer, E. Alberta, T.R. Shrout, High Curie temperature perovskite BiInO$_3$–PbTiO$_3$ ceramics, J. Mater. Res. 19 (2004) 2185–2193.
[9] D.Q. Shen, X.Z. Li, Z.J. Wang, Y. Liu, C. He, T. Li, H. Tailor, X.F. Long, Preparation and characterization of $(1 − x)$Pb(Lu$_{1/2}$Nb$_{1/2}$)O$_3$–xPbTiO$_3$ binary ferroelectric ceramics with high Curie temperature, Mater. Lett. 84 (2012) 1–4.
[10] I. Grinberg, M.R. Suchomel, P.K. Davies, A.M. Rappe, Predicting morphotropic phase boundary locations and transition temperatures in Pb- and Bi-based perovskite solid solutions from crystal chemical data and first-principles calculations, J. Appl. Phys. 98 (2005) 094111.
[11] C.J. Stringer, T.R. Shrout, C.A. Randall, I.M. Reaney, Classification of transition temperature behavior in ferroelectric PbTiO$_3$–Bi(Me′Me″)O$_3$ solid solutions, J. Appl. Phys. 99 (2006) 024106.
[12] L. Shi, Q.W. Liao, B.P. Zhang, J.Y. Zhang, D. Guo, Structure and electrical properties of $(1 − x)$(0.1BiYbO$_3$–0.9PbTiO$_3$)–xPb(Zn$_{1/3}$Nb$_{2/3}$)O$_3$ high-temperature ternary piezoelectric ceramics, Mater. Lett. 114 (2014) 100–102.
[13] L. Mitoseriu, C.E. Ciomaga, V. Buscaglia, L. Stoleriu, D. Piazza, C. Galassi, A. Stancu, P. Nanni, Hysteresis and tunability characteristics of Ba(Zr,Ti)O$_3$ ceramics described by first order reversal curves diagrams, J. Eur. Ceram. Soc. 27 (2007) 3723–3726.
[14] S.J. Zhang, E.F. Alberta, R.E. Eitel, C.A. Randall, T.R. Shrout, Elastic, piezoelectric, and dielectric characterization of modified BiScO$_3$–PbTiO$_3$ ceramics, IEEE Trans. Ultrason. Ferroelectr. Freq. Control 52 (2005) 2131–2139.
[15] J. Ryu, S. Priya, K. Uchino, High-T_m relaxor ferroelectrics: 0.3BiScO$_3$–0.6PbTiO$_3$–0.1Pb(Mn$_{1/3}$Nb$_{2/3}$)O$_3$, Appl. Phys. Lett. 82 (2003) 251–253.
[16] Z.H. Yao, H.X. Liu, M.H. Cao, H. Hao, Z.Y. Yu, Effects of Mn doping on the structure and electrical properties of high-temperature BiScO$_3$–PbTiO$_3$–Pb(Zn$_{1/3}$Nb$_{2/3}$)O$_3$ piezoelectric ceramics, Mater. Res. Bull. 46 (2011) 1257–1261.
[17] Q.W. Liao, X.S. Chen, X.C. Chu, F. Zeng, D. Guo, Effect of Fe doping on the structure and electric properties of relaxor type BSPT–PZN piezoelectric ceramics near the morphotropic phase boundary, Sens. Actuators A: Phys. 201 (2013) 222–229.
[18] F. Gao, Z.Q. Deng, L. Yang, L.H. Cheng, C.S. Tian, Phase transitional behavior and piezoelectric properties of BiYbO$_3$–Pb(Ti$_{0.5}$Zr$_{0.5}$)O$_3$–LiNbO$_3$ ceramics, Ceram. Int. 35 (2009) 2885–2890.

[19] J. Fu, R.Z. Zuo, X.H. Wang, L.T. Li, Phase transition characteristics and piezoelectric properties of compositionally optimized alkaline niobate based ceramics, J. Alloys Compd. 486 (2009) 790–794.

[20] R. Shannon, Revised effective ionic radii and systematic studies of interatomic distances in halides and chalcogenides, Acta Crystallogr. A 32 (1976) 751–767.

[21] B.S. Li, G.R. Li, Q.R. Yin, Z.G. Zhu, A.L. Ding, W.W. Cao, Pining and depinning mechanism of defect dipoles in PMnN–PZT ceramics, J. Phys. D: Appl. Phys. 38 (2005) 1107–1111.

[22] L.X. Zhang, X. Ren, In situ observation of reversible domain switching in aged Mn-doped $BaTiO_3$ single crystals, Phys. Rev. B 71 (2005) 174108.

[23] M. Budimir, D. Damjanovic, N. Setter, Enhancement of the piezoelectric response of tetragonal perovskite single crystals by uniaxial stress applied along the polar axis: a free-energy approach, Phys. Rev. B 72 (2005) 064107.

[24] M.D. Maeder, D. Damjanovic, C. Voisard, N. Setter, Piezoelectric properties of $SrBi_4Ti_4O_{15}$ ferroelectric ceramics, J. Mater. Res. 17 (2002) 1376–1384.

Biographies

Feng Jiang received her M.S. degree from Lanzhou Institute of Chemical Physics, Chinese Academy of Sciences, in 2010, and Ph.D. degree from Institute of Chemistry, Chinese Academy of Sciences, in 2013. She is now working in Institute of Acoustics, Chinese Academy of Sciences. Her current research interests is on piezoelectric and ferroelectric materials.
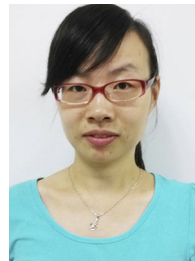
Yunli Wang received her Ph.D. degree from Shanghai Institute of Ceramics, Chinese Academy of Sciences, in 2013. She is now working in Institute of Acoustics, Chinese Academy of Sciences. Her current research is focused on piezoelectric and ferroelectric materials.

Junying Zhang received her B.S. degree (1996) and M.S. degree (1999) from University of Science and Technology Beijing and Ph.D. degree (2002) from Tsinghua University. She joined Beihang University (BUAA) in 2002 and became a Professor in 2009. Her scientific interest is focused on first-principles calculation and controllable synthesis of functional materials, photocatalytic materials for energy conversion and environmental remediation, luminescent materials for lighting and displaying.

Kai Cai received the Ph.D. degree in Department of Materials Science and Engineering in Tsinghua University, Beijing, China, in 2003. From 2003 to 2007, she was working on various ceramic and thin films in Tokyo Institute of Technology and the University of Tokyo, Japan. Her current research interests are on the characterization of various materials and materials characterization by using Transmission Electron Microscopy.

Dong Guo received the Ph.D. degree in Department of Materials Science and Engineering in Tsinghua University, Beijing, China, in 2003. From 2003 to 2007, he worked continuously on organic thin films of both small molecules and polymer and relevant devices in Tokyo Institute of Technology (JST postdoctoral researcher), the University of Tokyo and National Institute for Materials Science (NIMS) in Japan. From 2007 to 2009, he was a foreigner scientist at the Ceramics Laboratory of Swiss Federal Institute of Technology at Lausanne (EPFL). In 2010, he joined in Institute of Acoustics, Chinese Academy of Sciences, as a 'Hundred Talents Program' Professor. He is the leader of the 'Functional Materials Group' of the institute, and the current research of his group is focused on various piezoelectric, ferroelectric and semiconductive materials, and their application in various devices.